

DTIC FILE COPY

AD-A191 751

REPORT DOCUMENTATION PAGE

UNCLASSIFIED		12. RESTRICTIVE MARKINGS	
2a. SECURITY CLASSIFICATION AUTHORITY		3. DISTRIBUTION/AVAILABILITY OF REPORT	
2i. DECLASSIFICATION/DOWNGRADING SCHEME		Approved for public release; distribution is unlimited.	
4. PERFORMING ORGANIZATION REPORT NUMBER(S)		5. MONITORING ORGANIZATION REPORT NUMBER(S)	
6a. NAME OF PERFORMING ORGANIZATION	6b. OFFICE SYMBOL (if applicable)	7a. NAME OF MONITORING ORGANIZATION	
Naval Ocean Systems Center	NOSC	Naval Ocean Systems Center	
6c. ADDRESS (City, State and ZIP Code)		7b. ADDRESS (City, State and ZIP Code)	
San Diego, CA 92152-5000		San Diego, CA 92152-5000	
8a. NAME OF FUNDING/SPONSORING ORGANIZATION	8b. OFFICE SYMBOL (if applicable)	9. PROCUREMENT INSTRUMENT IDENTIFICATION NUMBER	
Naval Sea Systems Command	NAVSEA		
8c. ADDRESS (City, State and ZIP Code)		10. SOURCE OF FUNDING NUMBERS	
San Diego, CA 92152-5000		PROGRAM ELEMENT NO.	PROJECT NO.
		61153N	HM01
		TASK NO.	AGENCY ACCESSION NO.
		SR0230103	DN530 687
11. TITLE (Include Security Classification)			
A Propeller Skew Optimization Method			
12. PERSONAL AUTHOR(S)			
T.S. Mautner			
13a. TYPE OF REPORT	13b. TIME COVERED	14. DATE OF REPORT (Year, Month, Day)	15. PAGE COUNT
Professional paper	FROM Oct 1987 TO Oct 1987	November 1987	
16. SUPPLEMENTARY NOTATION			
17. COSATI CODES		18. SUBJECT TERMS (Continue on reverse if necessary and identify by block number)	
FIELD	GROUP	SUB-GROUP	turbulence injection, vortex shedding
			blade-passage frequencies and harmonics, blade-rate
19. ABSTRACT (Continue on reverse if necessary and identify by block number)			
<p>A propeller operating in the turbulent wake of an axisymmetric body with appendages encounters wake non-uniformities which result in spatial and temporal fluctuations of blade angle-of-attack. These angle-of-attack fluctuations result in unsteady blade loadings and the generation of propeller noise, and the noise sources are characterized by three types of unsteady force mechanisms: a) turbulence injection; b) vortex shedding; and c) blade-rate. The first two mechanisms typically generate continuous spectrum (broadband) radiated noise levels while blade-rate forces generate discrete frequency noise levels at various blade-passage frequencies and harmonics. This paper will address the reduction of blade-rate noise. (A.t) 5 The hull boundary layer behind an appendage (i.e. figure 1) is characterized by a complex velocity field typically having velocity excesses at inner radii and velocity deficits at the outer radii. This type of velocity field has a complex harmonic content and its effect on blade-rate noise cannot be predicted without detailed examination of the wake and the radial distribution of propeller blade forces. The reduction of blade-rate noise and thus vehicle vibration provides the motivation for the application of skew in propeller design.</p> <p>(Continued on page 2)</p>			
20. DISTRIBUTION/AVAILABILITY OF ABSTRACT		21. ABSTRACT SECURITY CLASSIFICATION	
<input type="checkbox"/> UNCLASSIFIED/UNLIMITED <input checked="" type="checkbox"/> SAME AS RPT <input type="checkbox"/> DTIC USERS		UNCLASSIFIED	
22a. NAME OF RESPONSIBLE INDIVIDUAL		22b. TELEPHONE (include Area Code)	22c. OFFICE SYMBOL
T.S. Mautner		619-226-2497	Code 634

DTIC ELECTED MAR 18 1988

88 3 16 055

*Un published versions
minor revisions to be
made*

A PROPELLER SKEW OPTIMIZATION METHOD

Thomas S. Mautner, Ph.D.
Hydromechanics Branch, Code 634
Naval Ocean Systems Center
San Diego, CA 92152

*use all
info for
abstract*

INTRODUCTION

A propeller operating in the turbulent wake of an axisymmetric body with appendages encounters wake non-uniformities which result in spatial and temporal fluctuations of blade angle-of-attack. These angle-of-attack fluctuations result in unsteady blade loadings and the generation of propeller noise, and the noise sources are characterized by three types of unsteady force mechanisms: a) turbulence injection; b) vortex shedding; and c) blade-rate. The first two mechanisms typically generate continuous spectrum (broadband) radiated noise levels while blade-rate forces generate discrete frequency noise levels at various blade-passage frequencies and harmonics. This paper will address the reduction of blade-rate noise. [A .ti 5 The hull boundary layer behind an appendage (i.e. figure 1) is characterized by a complex velocity field typically having velocity excesses at inner radii and velocity defects at the outer radii. This type of velocity field has a complex harmonic content distribution and its effect on blade-rate noise cannot be predicted without detailed examination of the wake and the radial distribution of propeller blade forces. The reduction of blade-rate noise and thus vehicle vibration provides the motivation for the application of skew in propeller design.

Techniques are available to computing unsteady forces and skew distributions, and these methods range from low-aspect ratio approximations to unsteady airfoil theory to complete unsteady, lifting-surface methods. However, since, no method was available to systematically determine an optimum skew distribution, the propeller skew optimization program SKEWOPT (Greenblatt, 1978; and Parsons and Greenblatt, 1978) was developed. SKEWOPT determines a quadratic or cubic skew distribution using an optimization technique which finds the set of parameters for which a user-defined linear combination of the unsteady force and moment amplitudes are minimized. SKEWOPT was written for use in ship propeller design; however, the intention was that, after minor modifica-

OR

Codes

Avail and/or
Special

A-1



tions such as the inclusion of higher order harmonic groups, it would be suitable for torpedo and submarine propeller design. Since the force calculation method in SKEWOPT was not sufficiently documented, the method was replaced, and, due to the difficulties encountered in modifying SKEWOPT, a new program, patterned after SKEWOPT, was written.

THE SKEW OPTIMIZATION PROBLEM

VELOCITY FIELD

Figure 1 shows one quadrant of a wake behind an axisymmetric body having four identical control surfaces. The spatial variations in the circumferential and radial directions are due to both potential and viscous effects, and it is this type of velocity field that plays an important part in the design of wake-adapted propellers. While circumferentially averaged velocity profiles can be used for propeller design calculations, the determination of a skew distribution, for the reduction of unsteady forces, requires that the spatial variations of the inflow velocity field be considered. Since the spatial velocity distributions are periodic and continuous, they may be represented in terms of a Fourier series or a complex exponential. For example, the axial component of the velocity at a position (r, θ) can be expressed as

$$\frac{U(r, \theta)}{U_\infty} = \frac{a_0(r)}{2} + \sum_{n=1}^{\infty} \left[a_n(r) \cos(n\theta) + b_n(r) \sin(n\theta) \right] = \operatorname{Re} \left[\frac{a_0}{2} + \sum_{n=1}^{\infty} c_n e^{in\theta} \right] \quad (1)$$

where U_∞ is the free stream velocity, $a_0(r)$, $a_n(r)$, $b_n(r)$ and $c_n(r) = a_n(r) - ib_n(r)$ are the Fourier coefficients and $\operatorname{Re} ()$ denotes the real part (only the real part will be used). Since, the term a_0 does not vary in θ , it is associated with the steady state thrust and torque, and the additional terms are sinusoidal fluctuations of the inflow velocity which produce the unsteady forces and moments.

Once the velocity field and propeller geometry are determined, the problem of determining an optimum skew distribution requires the formulation of a nonlinear programming problem which includes an unsteady force calculation method. First, the calculation of the unsteady forces will be considered.

UNSTEADY FORCE CALCULATION METHOD

The original version of SKEWOPT (Greenblatt, 1978) had both a two-dimensional, unsteady and a more time consuming lifting-line method available to calculate blade forces. To overcome computational problems, the original SKEWOPT force calculation methods were replaced by a method developed by Thompson (1976). Briefly, his method divides the propeller blade into strips which are considered two-dimensional airfoils. Included in the method are a) the two-dimensional unsteady airfoil theories of Sears (1941) and Horlock (1968) which allow consideration of sinusoidal velocity fluctuations normal and parallel to the inflow velocity, and b) corrections to the blade lift force due to the presence of adjacent propeller blades. The effect of blade camber (from Naumann and Yeh, 1973) has also been added.

In order to reduce blade-rate propeller forces, six unsteady forces and moments must be considered. As shown in figure 2, they are the thrust F_z , the side forces F_x and F_y , the torque T_z , and the bending moments T_x and T_y . For an axisymmetric body, one is not concerned with differentiating between the x and y components of the side forces and bending moments; therefore, the two side forces and bending moments were combined to yield the maximum side force, F_s , and maximum bending moment, T_s . The derivation of the force calculation method and extensions are given in Thompson (1976) and Mautner and Blaisdell (1987).

It has been shown (Thompson, 1976) that only certain inflow harmonics contribute to the unsteady forces and moments. They are the harmonics for which the order is some multiple (m) of the number of blades (N_b). Harmonics of order mN_b , gives rise to an unsteady force and moment in the z direction, F_z and M_z , while the side forces, F_x and F_y , and bending moments, M_x and M_y , are generated by inflow harmonics of order $mN_b \pm 1$. The equations for the thrust, torque and maximum side force and bending moment, for a given harmonic group m, are

$$F_s^{(m)} = N_b \left| \sum_{j=1}^P \left[L_{j(mN_b)} \right]_1 e^{-imN_b\psi} \right| \quad (2)$$

$$T_s^{(m)} = N_b \left| \sum_{j=1}^P \left[L_{j(mN_b)} \right]_1 r_j \tan(\beta_j) e^{-imN_b\psi} \right| \quad (3)$$

$$F_s^{(m)} = \frac{1}{2} N_b \left| \sum_{j=1}^P \left[L_{j(mN_b+1)} \right]_1 \tan(\beta_j) e^{-imN_b\psi} \right| + \frac{1}{2} N_b \left| \sum_{j=1}^P \left[L_{j(mN_b-1)} \right]_1 \tan(\beta_j) e^{-imN_b\psi} \right| \quad (4)$$

$$T_s^{(m)} = \frac{1}{2} N_b \left| \sum_{j=1}^P \left[L_{j(mN_b+1)} \right]_1 r_j e^{-imN_b\psi} \right| + \frac{1}{2} N_b \left| \sum_{j=1}^P \left[L_{j(mN_b-1)} \right]_1 r_j e^{-imN_b\psi} \right| \quad (5)$$

where L is the lift force, ψ is the skew, P is the number of blade strips, β is the pitch angle and the index m includes harmonic groups $m=1,2,3,4$. It should be noted that the contributions of the different harmonic groups are given separately since the unsteady forces due to different harmonic groups fluctuate at the frequencies $mN_b\Omega$ where Ω is the propeller rotation rate.

SKREW OPTIMIZATION MODEL

To determine the optimum skew distribution the above force calculation method has been incorporated into a nonlinear programming problem. Due to the fact that, in general, all forces cannot be minimized simultaneously, a scalar cost function formed from the weighted, linear combination of the forces and moments is minimized. The cost function F_c is

$$F_c = \sum_{m=1}^4 \left[\frac{W_1^{(m)} F_s^{(m)}}{.05 \bar{F}_s} + \frac{W_2^{(m)} F_s^{(m)}}{.05 \bar{F}_s} + \frac{W_3^{(m)} T_s^{(m)}}{.05 \bar{T}_s} + \frac{W_4^{(m)} T_s^{(m)}}{.05 \bar{T}_s} \right] \quad (6)$$

where the weights, W_j , are normalized such that their sum over both m and j ($=1, \dots, 4$) equals 1.

Since the F_c depends upon the skew distribution, $\psi(r)$, one could solve for the optimum skew via a variational or n dimensional parameter optimization technique. However, a more feasible approach, and the one used here, is to use a few parameters in describing the skew and perform an optimization search in a limited parameter space. To accomplish this, the skew distribution is represented by either a cubic or quadratic distribution having a straight line section with $\psi=0$. The

distributions (see Geenblatt, 1978 and Mautner and Blaisdell, 1987) are

$$\begin{aligned} \psi(r) &= ar^3 + br^2 + cr + d \quad \text{or} \quad br^2 + cr + d & r_h \leq r \leq r_t \\ \psi(r) &= 0 & r_h \leq r \leq r_s \end{aligned} \quad (7)$$

where r_h is the hub radius, r_t is the tip radius and r_s is the radius at which the polynomial skew distribution starts. This type of skew distribution is illustrated in figure 3.

The skew distribution given by equation (7) has five free parameters (a, b, c, d, r_s); however, it is more meaningful to the propeller designer to use parameters that have physical meaning instead of using these polynomial coefficients. The parameters chosen for use in the current method are the skew at the propeller tip ψ_t , the starting skew slope $S_s = \psi'(r_s)$, the starting radius r_s , and the skew slope at the tip S_t . Additionally, the physical restriction that $\psi(r_s) = 0$ is made so that the skew distribution is continuous thereby reducing the number of free parameters by one. Another necessary restriction is that the skew distribution be smooth which implies that $S_s = \partial\psi(r_s)/\partial r = 0$ if $r_s > r_h$. If there is no straight line section $r_s = r_h$, S_s is not restricted but r_s is fixed. In either case, the number of free parameters is reduced to three for a cubic distribution and two for a quadratic distribution and results in the four possible skew distribution models presented in table 1. Specification of these models allows the optimization search to be carried out in either a two or three dimensional space.

The propeller skew distribution problem has now been formulated as an optimization problem in terms of a few geometric parameters. In order to obtain a feasible propeller geometry, it is necessary to place some restrictions, such as a maximum allowable tip skew, on the geometric parameters. In doing so, the design problem becomes a constrained, nonlinear optimization problem where the optimization search is restricted to finding the set of parameters which minimizes the cost function F_c while satisfying all of the constraints placed on the problem. The constraints used are given in table 2 and are checked for violation at a given point in the parameter space. The additional constraint that the propeller blade should not curve forward has been incorporated.

The constrained, nonlinear optimization problem is represented by

$$\min F_c(\underline{X}) \text{ subject to } G_j(\underline{X}) \geq 0 \quad (8)$$

where \underline{X} is a vector in parameter space which determines the skew distribution and $G_j(\underline{X})$ describes the constraints. There are many techniques for solving the unconstrained minimization problem (see Parsons, 1975); however, only a few methods attack the constrained problem directly. One useful technique is to convert the constrained problem into an unconstrained problem and then use an unconstrained optimization method. This can be accomplished with the use of an external penalty function which is added to a cost function whenever a constraint is violated (i.e. $G_j(\underline{X}) < 0$). The penalty function can be expressed as

$$P(\underline{X}, r_k) = F(\underline{X}) - r_k \sum_j \min [G_j(\underline{X}), 0] \quad (9)$$

and then an unconstrained optimization technique can then be applied to $P(\underline{X}, r_k)$. If no constraint is violated no penalty is added and the penalty function is the same as the cost function. Since the penalty added is proportional to the constraint violation, the optimization method should be forced towards a feasible region where no constraints are violated. This will be the case as long as the multiplicative factor r_k is large enough (≈ 1024). If r_k is too small, the search may tend toward an infeasible region. The optimization technique chosen for use in this method is the Nelder-Mead simplex search method (Nelder and Mead, 1965), and a detailed description of the method as coded in the current computer program is given by Mautner and Blaisdell (1987).

The computer program which solves the above nonlinear programming problem is an interactive program intended for routine propeller design work. The program has an interactive input method to accept propeller data and optimization parameters, and the program can be restarted, for example, with different constraint values. In addition to the optimization mode, a test mode is available for the calculation of unsteady forces for a given skew distribution.

SKEW DISTRIBUTION CALCULATIONS

To demonstrate the results that can be obtained from the current skew optimization program, the forward propeller of a counterrotating propeller set was used to calculate several optimum skew distributions. The propeller was designed using the velocity data measured, in a wind tunnel, by Nelson and Fogarty (1977) and the propeller design programs of Nelson (1972, 1975). The operating parameters and the unskewed blade geometry are given in table 3 and schematically shown in figure 2.

It has been mentioned that only certain harmonics of the inflow velocity field contribute to the unsteady forces and moments. Since the current propeller has six blades and is operating in a four cycle wake, only those harmonics which are integer multiples of the blade number N_b need be considered, and the forces of interest are the unsteady thrust, F_u , and torque, T_u . To provide the final set of data required for the skew calculations, a Fourier analysis of the input wake (figure 1) was performed. The results show, for the six bladed propeller, the dominance of the 12th harmonic and the rapid approach to a nearly zero magnitude of the 24th and higher harmonics (Mautner, 1987). The radial distribution of the 12th harmonic is plotted in figure 4.

The propeller geometry and the radial distribution of the 12th and 24th harmonics were used in determining the skew distributions given in figure 5 and the magnitude of the forces and moments presented in table 4. To provide a reference, the magnitude of the forces and moments for the unskewed propeller were calculated. Next, each of the four skew distribution models with the appropriate constraints (see tables 2 and 4) was specified. The actual values of the constraints and the resulting values of the total forces and moments are given in table 4, and the calculated skew distributions are plotted in figure 5.

It is clear from an examination of the magnitudes of the forces and moments given in table 4 that a significant reduction of the the total thrust and torque on the propeller was achieved regardless of the skew model used. It can also be seen that the degree of force reduction and the blade

tip skew varies with skew model with the quadratic #1 model producing the lowest force and moment values (>80% reduction) and the maximum tip skew (54°). The radial distribution of skew shown in figure 5 indicates close similarity in the results of each model and skew distributions which will yield satisfactory propeller geometries without severe restrictions being placed on the skew model constraints. Clearly, the choice of which model to use or what level of force reduction, maximum tip skew or propeller geometry is acceptable must be determined by the application. It should be mentioned that the actual magnitude of the force or moment is not as important as the relative force reduction from the unskewed to skewed propeller geometries.

CONCLUSION

Based on SKEWOPT, an enhanced skew optimization technique was developed. The current method provides a fast and efficient way to determine a variety of cubic or quadratic skew distributions which minimize the unsteady forces produced by the various harmonic components of the input wake. The method has been extended to include higher order harmonics, allows the investigation of force magnitudes due to individual harmonics and the calculation of forces for specified skew distributions. Since the program is interactive and involves relatively short computation times, it provides a valuable tool for propeller design.

ACKNOWLEDGEMENTS

This work was funded by the Torpedo Hydromechanics and Hydroacoustics Program of the Naval Sea Systems Command and the Naval Ocean Systems Center Independent Exploratory Development Program. I thank G. Blaisdell for his work on the original development and programming of the method.

REFERENCES

- Greenblatt, J.E., "SKEWOPT: A Propeller Skew Optimization Program, User's and Programmer's Documentation," Univ. of Michigan, Dept. of NAME Report No. 204, 1978.
- Horlock, J.H., "Fluctuating Lift Forces on Airfoils Moving Through Transverse and Chordwise Gusts," J. Basic Eng., 1968.
- Mautner, T.S. and Blaisdell G. A., A Propeller Skew Optimization Method, NOSC Tech. Report in Progress, 1987.

Naumann, H. and H. Yeh, "Lift and Pressure Fluctuations of a Cambered Airfoil Under Periodic Gusts and Applications in Turbomachinery," J. of Eng. and Power, Vol. 95, No. 1, 1973.

Nelder, J.A. and R. Mead, "A Simplex Method for Function Minimization," Computer Journal, Vol. 7, No. 4, 1965.

Nelson, D.M., Development and Application of a Lifting Surface Design Method for Counterrotating Propellers, NUC TP 326, 1972.

Nelson, D.M., A Computer Program Package for Designing Wake-Adapted Counterrotating Propellers: A User's Manual, NUC TP 494, 1975.

Nelson, D.M. and Fogarty, J.J., Private Communication, 1977.

Parsons, M.G., "Optimization Methods for Use in Computer-Aided Ship Design," Proceedings of the First Ship Technology and Research (STAR) Symposium, Washington, D.C., 1975.

Parsons, M.G. and J.E. Greenblatt, "Optimization of Propeller Skew Distribution to Minimize the Vibratory Forces and Moments Acting at the Propeller Hub," Univ. of Michigan, Dept. of NAME Report No. 206, 1978.

Sears, W.R., "Some Aspects of Non-Stationary Airfoil Theory and Its Practical Application," J. Aero. Sciences, Vol. 8, No. 3, 1941.

Thompson, D.E., "Propeller Time-Dependent Forces Due to Nonuniform Flow," Applied Research Laboratory, Pennsylvania State Univ., Tech. Mem. TM No. 76-48, 1976.

Table 1. Skew Distribution Models.

Model	Type	Free Parameters	Fixed Parameters
1	Quadratic	ψ_t, S_0	$r_s = r_h$
2	Quadratic	ψ_t, r_s	$S_0 = 0$
3	Cubic	ψ_t, S_0, S_2	$r_s = r_h$
4	Cubic	ψ_t, S_0, r_s	$S_2 = 0$

Table 2. Skew Distribution Constraints

Constraint	Parameters
Skew Start Radius	$r_h \leq r_s \leq r_t$
Tip Skew	$\psi_{t,min} \leq \psi_t \leq \psi_{t,max}$
Skew At Any Radius	$\psi_{min} \leq \psi(r) \leq \psi_{max}$
Start Skew Slope	$S_{0,min} \leq S_0 \leq S_{0,max}$
Slope At Any Radius	$\psi'_{min} \leq \psi'(r) \leq \psi'_{max}$

Table 3. QT Propeller Geometry and Operating Characteristics

Number of Blades	N_b	6
Propeller Radius (ft)	R	0.683
Hub Radius (ft)	r_h	0.287
Propeller Rotation	RPM	1400
Vehicle Speed (fps)	U_∞	72.6

r Radius (ft)	$\frac{1}{2}C$ Semi-Chord (ft)	β Pitch (rad)	V_{tip}/V_∞ Rel. Velocity
0.296851	0.114494	0.565045	0.720017
0.316671	0.122523	0.591346	0.792238
0.336491	0.130216	0.523094	0.862482
0.356310	0.137558	0.643439	0.929732
0.376130	0.144531	0.659396	0.991884
0.395949	0.151114	0.679998	1.049763
0.415769	0.157285	0.700093	1.103771
0.435589	0.163010	0.712838	1.155713
0.455408	0.168254	0.715692	1.206251
0.475228	0.172969	0.711126	1.255548
0.495047	0.177082	0.702491	1.303797
0.514867	0.180495	0.691375	1.351201
0.534687	0.183012	0.678054	1.397928
0.554506	0.183925	0.662369	1.444151
0.574326	0.182208	0.643210	1.490022
0.594145	0.176667	0.619413	1.536311
0.613965	0.165930	0.590724	1.581767
0.633784	0.148949	0.563650	1.625661
0.653604	0.124835	0.544594	1.668754
0.673424	0.092792	0.518522	1.711513

Table 4. Calculated Total, Unsteady Thrust and Torque and Mid-Chord Tip Skew.

Skew Model (see Table 1)	$mN_b=12$		$mN_b=24$		Skew ϕ
	F_s^*	T_s^*	F_s^*	T_s^*	
No Skew	38.2	15.4	14.1	5.9	0.0
Quadratic #1	1.1	0.2	2.4	0.7	54.0
Quadratic #2	8.4	3.0	3.3	0.9	38.3
Cubic #3	2.6	0.9	1.9	0.3	44.6
Cubic #4	3.1	1.1	1.8	0.4	48.0

Constraints.
 Maximum Tip Skew - 60°
 Minimum Tip Skew - -30°
 Maximum/Minimum Skew Slope - ±5.28
 Maximum Start Radius - 0.683
 Minimum Start Radius - 0.287

Notes
 * Units (Force (thrust)-lbs; (T)orque-ft-lbs
 ** Mid-chord tip skew - deg

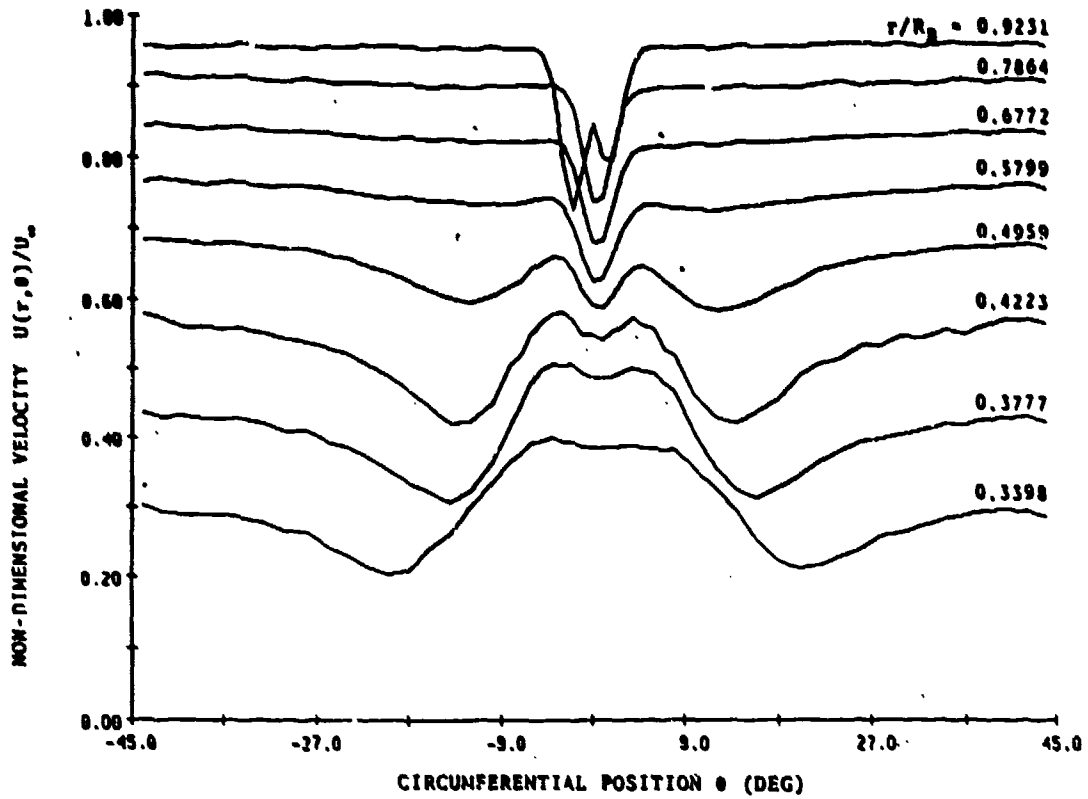


FIGURE 1. CIRCUMFERENTIAL VARIATION OF THE MEASURED INFLOW VELOCITY FIELD

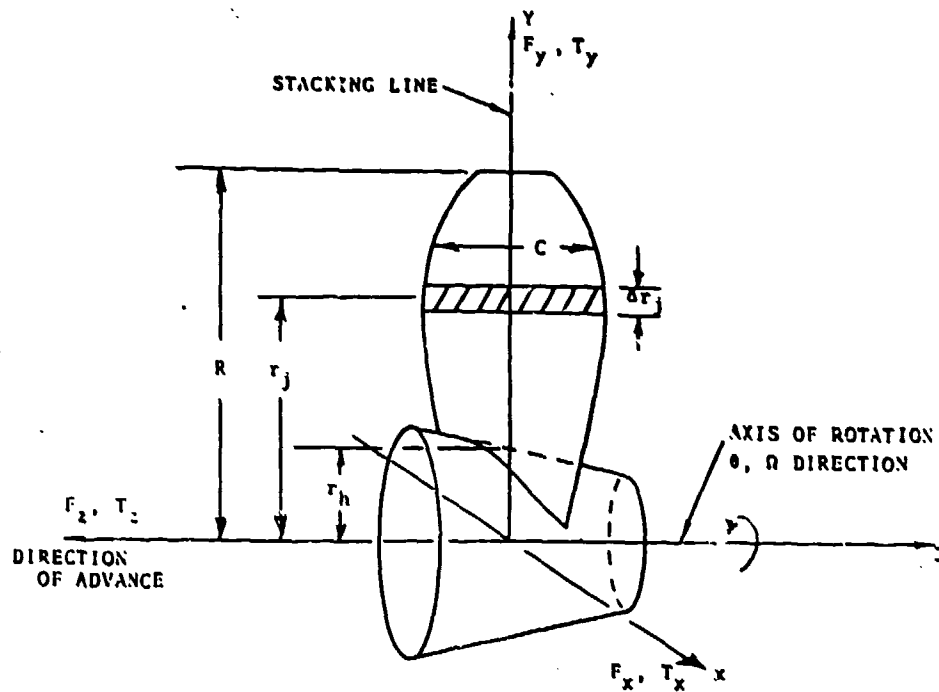


FIGURE 2. DESCRIPTION OF A TYPICAL PROPELLER AND ITS GEOMETRY

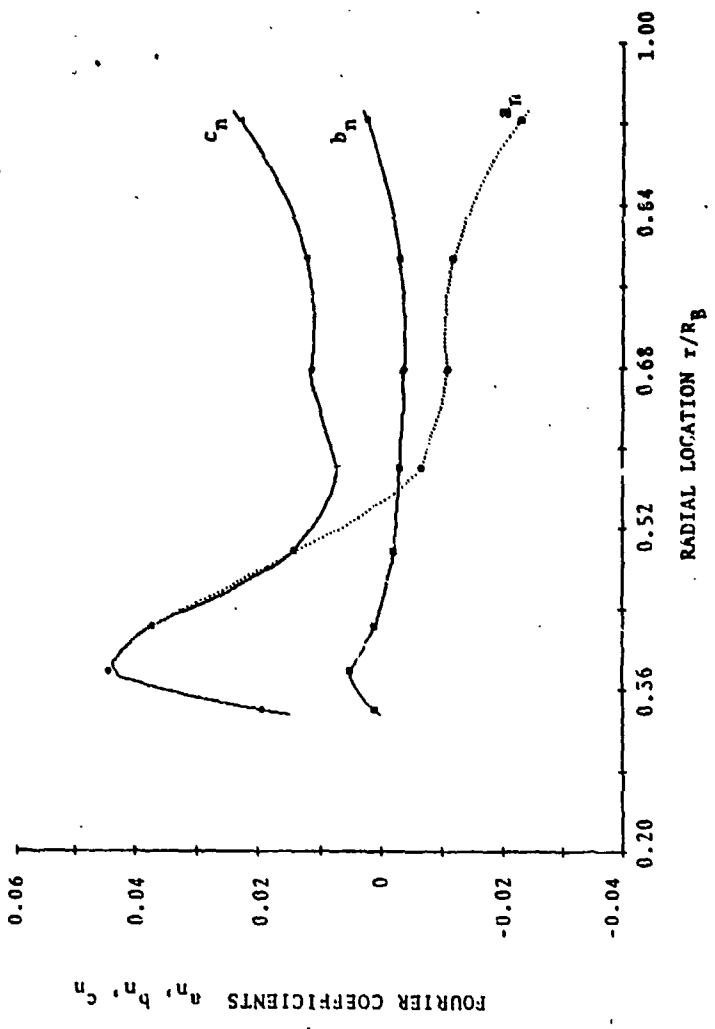


FIGURE 4. VARIATION FOURIER COEFFICIENT AMPLITUDE WITH RADIAL POSITION FOR THE 12TH HARMONIC

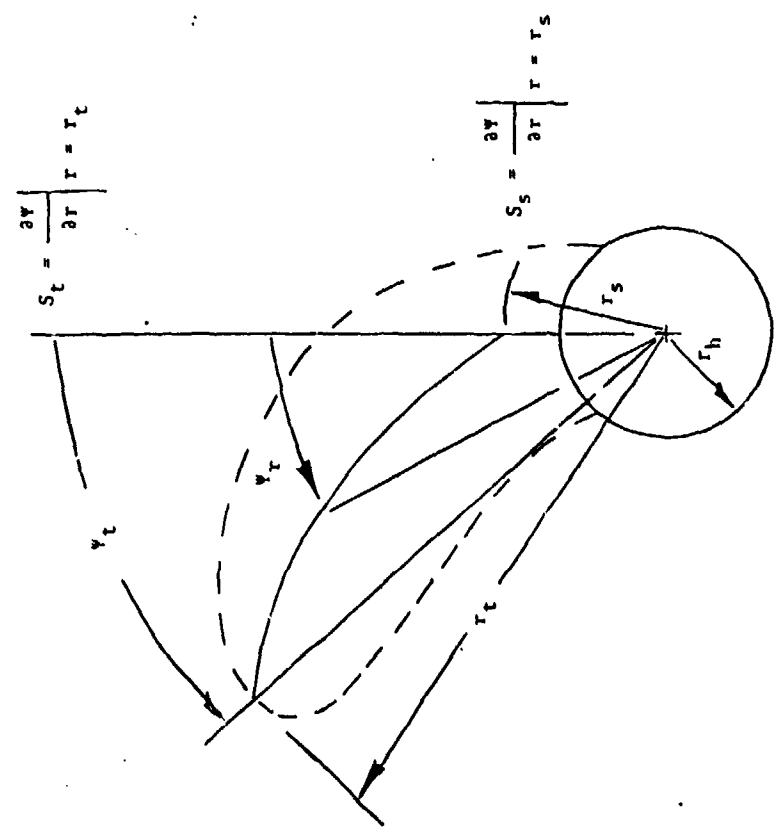


FIGURE 3. DEFINITION OF SKEW DISTRIBUTION MODEL PARAMETERS

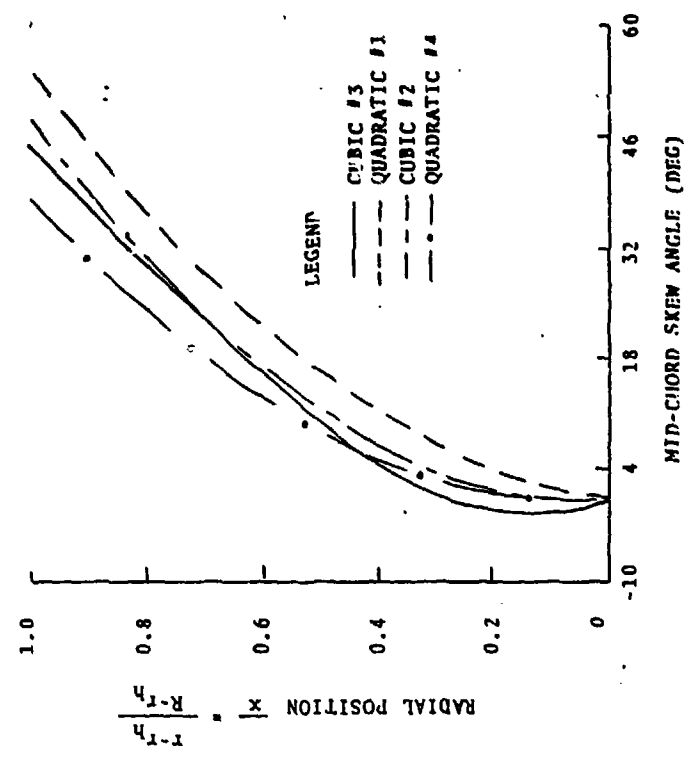


FIGURE 5. CALCULATED OPTIMUM MID-CHORD SKEW